Marine Biology (2024) 171:207
https://doi.org/10.1007/s00227-024-04531-1

ORIGINAL PAPER

Ups and downs: copepods reverse the near-body flow to cruise in the water column

Nils B. Tack[1] · Sara Oliveira Santos[1] · Brad J. Gemmell[2] · Monica M. Wilhelmus[1]

Received: 4 August 2024 / Accepted: 26 September 2024 / Published online: 10 October 2024

Abstract

Copepods are negatively buoyant organisms actively participating in large-scale vertical migrations as primary consumers in marine ecosystems. As such, these organisms need to overcome their own weight to swim upwards, incurring extra energy costs that are not offset by any mechanism intrinsic to drag-based propulsion. While copepod vertical migrations are well documented, it is still unclear how they achieve extensive upward cruising despite this limitation. In this study, we found suction to be a compensatory mechanism enhancing thrust in upward-swimming copepods. Using experimentally derived velocity and pressure fields, we observed that copepods pull water in front of them to generate sub-ambient pressure gradients when cruising upward, thereby inducing an upstream suction force to complement the thrust produced by the legs. Contrary to expectations that drag always dominates the leg recovery phase, we found that the upstream suction generates net thrust for about a third of the recovery stroke. In contrast, downward-swimming copepods push rather than pull on water and do not benefit from thrust-enhancing suction effects during the recovery stroke. Differences in the induced flows are associated with contrasting leg kinematics, indicating a response to the body orientation rather than a fixed effect. These results offer insights into an important swimming mechanism that can inform the role mesozooplankton play in biogenic hydrodynamic transport and its impact on marine biogeochemistry.

Keywords Copepod · Vertical cruising · Pressure fields

Introduction

Copepods are one of the most abundant mesozooplankton in marine ecosystems (Humes 1994). Despite their small size (≈200–2000 µm), many copepod species take part in large-scale mass movements known as diel vertical migrations (DVM), which are central to their ecological role as primary consumers (Gauld 1953; Roe 1972; Conroy et al. 2020). They cover vertical distances of up to several hundred meters to forage in shallow waters (Bianchi et al. 2013; Bianchi and Mislan 2016). Vertically migrating mesozooplankton have a complex role in biogeochemical cycling, notably the biological pump regulating carbon transport from primary producers at the surface into the deep ocean (reviewed in (Steinberg and Landry 2017; Cavan et al. 2019). Considering translocating organism-level functions alone (such as grazing and excretion), DVM-mediated transport of organic matter has been estimated to contribute 14–40% of the global export flux, along with redistributing oxygen profiles (Bianchi et al. 2013; Aumont et al. 2018; Archibald et al. 2019). Vertical migrations have thus been hypothesized to potentially have important effects on the local-to-global biogeochemistry of the ocean (Wilhelmus and Dabiri 2014; Houghton et al. 2018; Houghton and Dabiri 2019; Wilhelmus et al. 2019; Siegel et al. 2023). To contextualize the relevance of copepods in oceanic ecosystems further, it is essential first to understand the swimming characteristics and hydromechanical mechanisms enabling the vertical relocation of individual plankton.

In free-swimming copepods, propulsion is governed by the combined action of four forces: thrust, drag, weight, and buoyancy. The flow field produced around a copepod,

Communicated by C. Meunier .

✉ Monica M. Wilhelmus
mmwilhelmus@brown.edu

[1] School of Engineering, Brown University, 345 Brook St, Providence, RI 02912, USA

[2] Department of Integrative Biology, University of South Florida, 4202 East Fowler Ave, Tampa, FL 33620, USA

responsible for thrust and drag, is controlled by several factors. Because copepods cruise in the transitional flow regime at Reynolds numbers (Re) $1 \leq Re \leq 100$, body shape determines the stress applied to the water along the body-fluid interface, inducing viscous and pressure drag during swimming. The motion patterns of the cephalic appendages also significantly impact the local flow by pulling water toward the animal, such as during feeding or pushing water away to generate drag-based thrust (Bundy and Paffenhöfer 1996; Malkiel et al. 2003). In negatively buoyant calanoid copepods, weight (due to the gravitational acceleration) is critical during vertical movements (Clarke 1934; Haury and Weihs 1976; Strickler 1982) given that its magnitude is comparable to the induced viscous drag forces (Svetlichny et al. 2020; Jiang 2023). The copepods excess weight (negative buoyancy) can have a significant impact on performance (i.e., swimming speed) depending on the swimming direction (Jiang 2023). On the one hand, cruisers swim faster going downwards by virtue of swimming in the direction of sinking, whereby drag is the only retarding force, and the terminal sinking velocity contributes partially to the overall downward swimming speed (Jiang 2002). On the other hand, to achieve hovering and upward swimming, copepods must at least generate forces that counterbalance the induced drag plus their excess weight (Jiang and Osborn 2004; Jiang 2023). Early flow visualization experiments hypothesized that copepods might take advantage of the additional work needed to overcome this excess weight resisting swimming (the gravitational acceleration being opposite to the swimming direction) to generate a comparatively stronger anterior velocity gradient pulling water toward the body (Strickler 1982; Emlet and Strathman 1985). While generating such anterior pulling flow enhanced prey detection and encounter (Tiselius and Jonsson 1990; Yen and Strickler 1996; Giuffre et al. 2019), its association with excess weight and role in propulsion remains unclear. The implications of the excess weight, in conjunction with drag, are that copepods need to generate more power during upward swimming, likely increasing the cost of transport (COT) (Marshall and Orr 1972; Jiang 2023). Without any other mechanism, this additional power demand creates a noticeable disparity in efficiency between upward and downward swimming.

Daily migrations are thought to be energetically expensive. Based on the observed duration and amplitude of DVMs of calanoid copepods, the physiological cost is estimated to range between 13% and 120% of the basal metabolic rate (reviewed in (Mauchline 1998). This wide range depends on the species, estimated swimming speed, swimming mode, and migration amplitude. How copepods perform extensive cruising despite energetic limitations has been thus far evaluated from an ecological standpoint, but hydrodynamic effects need to be considered. For instance, numerical simulations suggest that producing a strong, pulling anterior flow can enhance the prey capture volume to offset the energy budget of migration and satisfy the energy need of upward cruising (Jiang 2002). This argument is partly supported by the fact that grazing motivates upward swimming, especially during DVMs. However, in this context, compensating for, rather than mitigating, energy losses makes vertical swimming highly dependent upon unpredictable external factors, such as food density and abundance, with potentially undesired consequences.

From a bio-fluids perspective, an alternative explanation for the role of the strong velocity gradient produced by upward cruisers stems from how some animals *pull* themselves through the water using suction thrust (Colin et al. 2012; Gemmell et al. 2015, 2016). By accelerating the surrounding fluid — such as when pulling on water — counter-rotating vortices form at the interface of which a high-velocity, low-pressure region exists (Colin et al. 2012; Dabiri et al. 2020). The reciprocal action of this local low pressure anterior to the swimming appendage and body generates a suction force in the swimming direction, contributing to thrust (Gemmell et al. 2015). This pull-thrust mechanism promotes economical swimming and enhances performance in fish (Gemmell et al. 2015; Tack et al. 2021), jellyfish (Colin et al. 2012; Dabiri et al. 2020), and ctenophores (Colin et al. 2020). This is because the inertia carried by the persisting induced flow can be harnessed at no additional cost. Such a mechanism potentially offers negatively buoyant copepods an effective solution to overcome their excess weight when cruising vertically. We hypothesized that by setting up a strong persisting anterior flow during upward swimming, copepods harness similar suction effects to enhance thrust. Doing so would facilitate upward cruising by assisting the legs in generating the necessary thrust to counter their excess weight and the induced drag. In contrast, we expect downward swimmers to achieve greater cruising speeds but no longer benefit from their excess weight to generate a strong pulling force. The goal of this study is to evaluate the impact this mechanism has on thrust production and vertical cruising. Can copepods actively modulate the flow around their body in response to orientation when cruising in the water column? Our results establish a physical basis for the ecological success and distribution of small mesozooplankton swimmers whose large swarms during DVM potentially regulate the biogeochemistry of our ocean. More comprehensive studies are needed to further corroborate and advance our understanding of the physical processes of this ecologically-relevant species.

Materials and methods

Adult copepods *Temora longicornis* (prosome length BL = 0.6–0.8 mm) were collected in July 2020 from a pier in Woods Hole, Massachusetts, USA, and acclimated overnight at room temperature (≈21 °C). Observations were made in a small filming vessel (1 × 3 × 3 cm) containing a dilute suspension (3 to 5 copepods) such that the flow field of the observed local organism was not affected by that of other swimmers. The filming vessel was emptied and re-filled with a fresh suspension every time a recording was kept to prevent resampling of the same animal. Males and females were not differentiated at this stage. Experiments were conducted using 35‰ filtered seawater at 21 °C. Bright-field 2D-Particle Image Velocimetry (PIV) was performed following methods by (Gemmell et al. 2014). The water was seeded with heat-killed microalgae *Nannochloropsis oculata* (≈2 µm in diameter), backlit by a 150 W fiber optic illuminator (Fisher Scientific, Hampton, NH, USA) coupled with a collimating lens to visualize the flow. The light source did not induce phototaxis. Free-swimming copepods were recorded dorsoventrally using a high-speed digital video camera (Fastcam Mini WX 100; Photron, Tokyo, Japan) at 2000 frames per second (1024 × 1024 pixels). Despite using volume illumination, the camera was equipped with a high-magnification optical set-up of a narrow depth-of-focus (DoF ≈ 127 µm, see supplementary materials). In total, dozens of videos were recorded, but it must be noted how challenging it is to capture a copepod in such a narrow 2D field for a significant period in an open 3D filming vessel away from walls. Sequences of upward and downward swimming were selected only when the copepods were fully in view and within the focal plane for several consecutive leg beats. In total, we studied four freely swimming copepods; two animals swimming upward ($0 < U < \pi$) and two specimens swimming downward ($-\pi < U < 0$) (see Table 1). The copepod population was female dominated and all four copepods reported in this study were females. Observations in which the copepods moved out of the focal plane or exhibited undesirable behaviors, such as jumping, were excluded from the analysis. Fluid velocity vectors were calculated using the DaVis 10 software package (LaVision, Göttingen, Germany). Image pairs were analyzed with three passes of overlapping interrogation windows (75%) of decreasing size of 48 × 48 pixels to 32 × 32 pixels. Manually masking the body of the copepods before image interrogation confirmed the absence of surface artifacts in the PIV measurements. All frames were used for analysis, yielding a separation between frames (Δt) of 5×10^{-4} s.

Morphometrics and swimming kinematics measurements were performed from the scaled PIV videos for each copepod using the ImageJ software (Schneider et al. 2012). The Reynolds number (Re) of each copepod was calculated as $\mathrm{Re} = \mathrm{BL}\, u / \nu$, where BL is the prosome length, u is the swimming speed, and ν is the kinematic viscosity for seawater at 21 °C and 35‰. The locomotor classification was determined for each animal after computing the velocity fields and was based on the direction of the dominant anterior flow. Motions of the second antennae (A2), the dominant propulsive cephalic appendages, were measured in degrees relative to the swimming direction U at the beginning and end of a power stroke and normalized to 180° (corresponding to the lateral halves of the body). Normalized angles equal to 0.5 indicate a lateral orientation, while angles < 0.5 and > 0.5 indicate anterior and posterior orientations, respectively. Kinematics parameters were averaged for several consecutive leg beats from the beginning of the video sequence to either the end of the sequence or when the copepod left the field of view (see Table 1). Note that other cephalic appendages, including the mandibles (Md), first

Table 1 Copepod morphometrics and swimming parameters. Parameters measured for each copepod over several consecutive appendage beats are reported as mean ± standard deviation. The copepod Reynolds number (Re) was calculated using the prosome length

Copepod ID	Copepod 5	Copepod 8	Copepod 1	Copepod 6
Locomotor classification	puller	puller	pusher	pusher
Prosome length (m)	6.34×10^{-4}	6.58×10^{-4}	7.76×10^{-4}	7.56×10^{-4}
Prosome width (m)	4.46×10^{-4}	4.52×10^{-4}	4.49×10^{-4}	4.41×10^{-4}
Re	0.93	2.96	7.37	6.02
Mean swimming speed (BL s^{-1})	2.37	6.99	12.54	10.78
Leg beat frequency (s^{-1})	57.69[b]	58.82[c]	57.69[d]	61.22[d]
Swimming direction (rad)	1.555	1.529	−1.327	−2.880
Cephalic appendages beat motion[a]	anterior–lateral	anterior– lateral	lateral–posterior	lateral–posterior
Relative anterior appendage start angle[a]	0.28 ± 0.01[b]	0.23 ± 0.01[c]	0.47 ± 0.04[d]	0.57 ± 0.02[d]
Relative anterior end angle	0.49[b]	0.60[c]	0.79[d]	0.71[d]

[a]Relative to the swimming direction and normalized to 180°

[b]Calculated for 7 consecutive leg beats

[c]Calculated for 10 consecutive leg beats

[d]Calculated for 3 consecutive leg beats

(Mx1) and second (Mx2) maxillae, and maxillipeds (Mxp) (see Fig. 1), were also beating during swimming but could not be tracked over time because they were obstructed by the prosome (due to the dorsoventral view). The antennules (A1) were not involved in locomotion. Stacking sequential images of a complete leg beat cycle (Photoshop 2024, Adobe, CA, USA) reveals the motions of the legs over time and their overall position relative to the body of the copepods (see Fig. 2).

Pressure fields around the body of the copepods were computed using the Queen 2.0 package for Matlab (Dabiri et al. 2014; Lucas et al. 2017). Given the sensitivity of this calculation to standard PIV errors at the fluid-solid interface, the copepod body shapes were manually masked before image interrogation, ensuring the absence of surface artifacts in the PIV measurements. While two-dimensional, this approach accurately estimates the pattern, timing, and magnitude of pressure fields around zooplankton (Colin et al. 2020). Note that the final pressure estimates are relative to a zero-reference pressure corresponding to the surrounding ambient pressure (gauge pressure).

Forces were computed from the pressure fields to quantify the contribution of positive and negative pressures to thrust and drag (Lucas et al. 2017). Force magnitude was calculated per unit depth (because PIV data were 2D) as the product of the length of each segment between points making up the outline of the copepod, the pressure along each segment, and the unit vector normal to each segment, giving units of Newtons per meter. Thrust and drag are the axial components of the forces in the swimming direction, U (see supplementary materials). Forces were classified as pull and push forces when arising from sub-ambient pressures (negative relative to ambient) and above-ambient pressures (positive), respectively. The forces produced over time were averaged for several consecutive beat cycles (see Table 1). Here, we also need to remind the reader that the results presented in this study are based on observations from four individuals of the same species: two swimming upward and two swimming downward. This small sample size, along with the focus on a single species, limits our ability to safely generalize our findings to other copepod species or broader ecological systems.

Results

The upward-swimming copepods swam nearly vertically (U was less than 3° offset from the vertical laboratory frame of reference). One of the downward-swimming copepods displayed a strong horizontal component (see Table 1, Supplementary S1). We determined this had little to no effect on their behavior because induced drag is the only force opposing their motion. We also confirmed the display of the cruising rather than the feeding behavior (or a combination

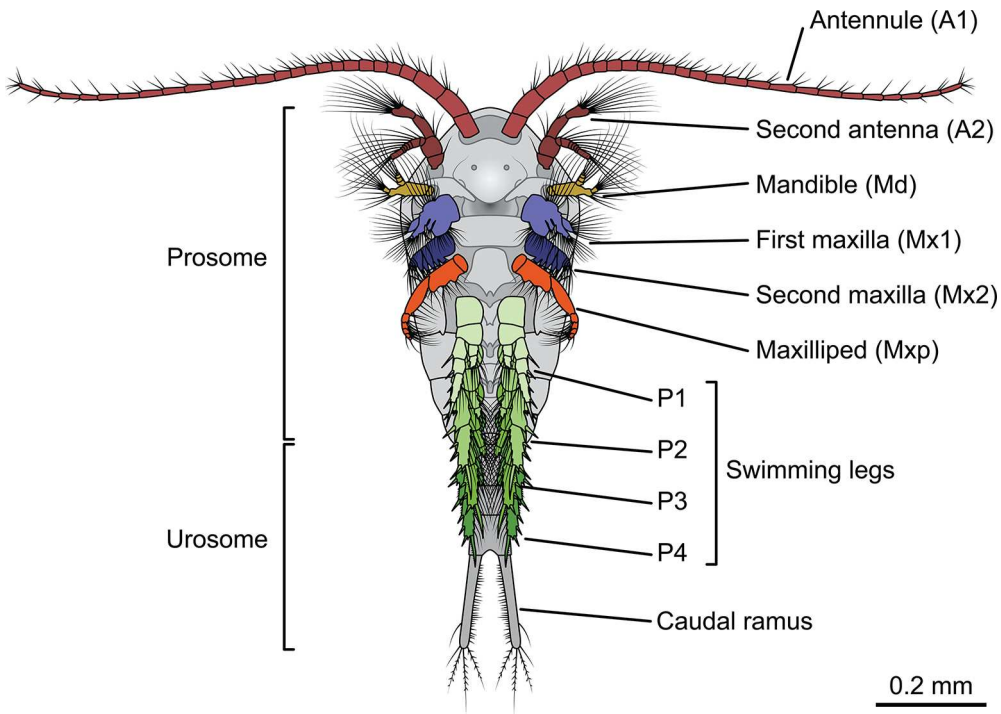

Fig. 1 *Temora longicornis* external morphology (ventral view). This view highlights the location of the five cephalic appendages employed during swimming in our experiments (A2, Md, Mx1, Mx2, and Mxp). Other swimming legs (P1–P4) are generally employed during fast swimming. Copepod length was measured as the prosome length

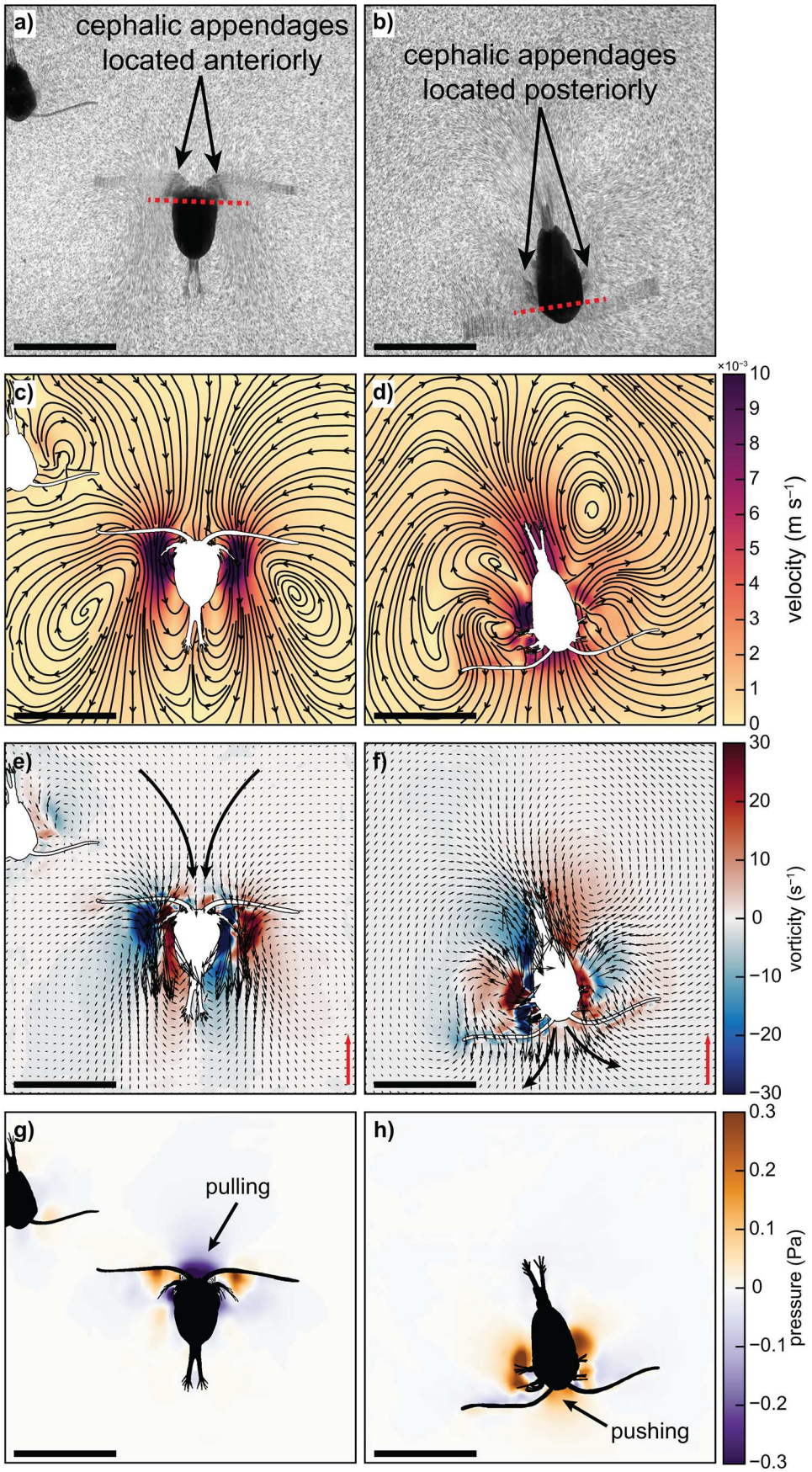

Fig. 2 Copepod-fluid interactions during upward and downward swimming. Image stacks of two representative copepods showing that upward swimmers (**a**) maintained their legs anterior to the body during a leg beat cycle (copepod ID: 8; stack length = 35 frames = 0.0175 s) while downward swimmers (**b**) maintained their legs posteriorly to the body (Copepod ID: 1; stack length = 35 frames = 0.0175 s). The red dashed lines in both panels pass through the widest portion of the body in the last frame of the stack to serve as a visual reference to locate the legs relative to the body. Instantaneous velocity magnitude and streamlines (in a lab-reference frame) of a slow, ascending (**c**), and a fast downward swimming copepod (**d**). Upward swimmers pull the water toward them, while downward swimmers push the water away. Instantaneous vorticity fields show the different flow characteristics of pullers (**e**) and pushers (**f**). Thick arrows indicate the dominant flow produced in front of the copepods. The red scale arrow in (**e**,**f**) indicates 1×10^{-2} m s^{-1}. Every three vectors were plotted for clarity. (**g**) Experimentally derived pressure fields show that copepods drop the pressure in front of them by pulling water in when ascending. (**h**) In contrast, downward swimming pushers generate a high-pressure area in front of them. The black scale bar indicates 1 mm in all the panels

thereof) with the absence of the characteristic kinematics and flow features commonly associated with the production of a feeding current (Cannon 1928; Strickler 1982, 1984) (see supplementary materials).

Both upward swimmers were slower than the downward cruisers. Upward swimmers had speeds $u = 2.37$ and 6.99 BL s^{-1}, while downward cruisers swam at $u = 12.54$ and 10.78 BL s^{-1} (Table 1). The terminal sinking speed ω_s of copepods can be expected to range from $\omega_s = 2.5$ to 2.9 mm s^{-1} (Apstein 1910; Tiselius and Jonsson 1990). Using a modified Stokes' law, we estimated for this species an $\omega_s = 2.68 \pm 0.05$ mm s^{-1}, equivalent to 3.82 ± 0.41 BL s^{-1} (see supplementary materials). While the drag coefficient may fluctuate in self-propelled organisms, thus giving only estimates of ω_s (Jiang 2023), knowing ω_s provides an estimate of the contribution of the terminal velocity to the overall observed swimming speed when moving downward. Indeed, ω_s of downward-swimming copepods is 27.8 and 32.0% of the measured vertical swimming velocity u for copepods 1 and 6, respectively.

In all cases, cruising was achieved using the same metachronal swimming mode by beating the cephalic appendages. Swimming upward induced *breaststroke* kinematics consisting of the cephalic appendages extending anteriorly

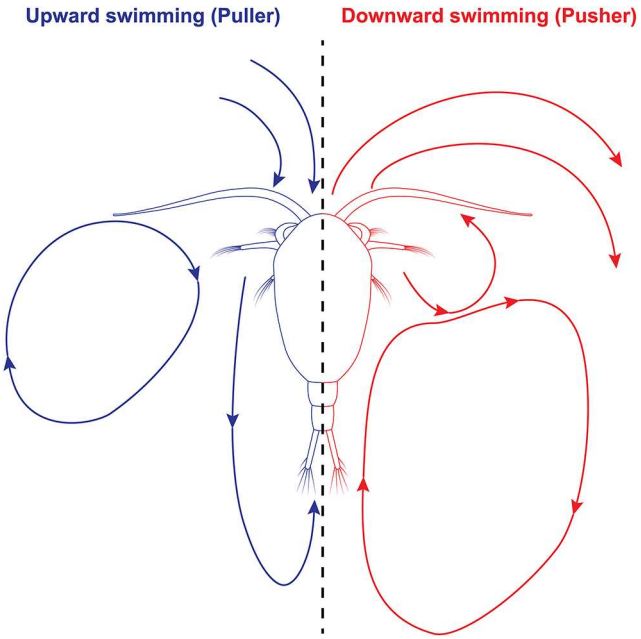

Fig. 3 Schematics of the near-field flow produced by downward and upward swimming copepods. Upward swimming copepods pull in a large funnel-like volume of water anteriorly that is expelled posteriorly in momentum jets (left). They produce two vortices on each side of the body; one large vortex adjacent to the prosome and another laterally compressed vortex extending posteriorly along the urosome. Downward swimmers push the water in front of them and also form two observable vortices (right). One small vortex surrounds all the cephalic appendages, and a much larger counter-rotating vortex is located posteriorly and extends far behind the urosome

at the beginning of the power stroke (normalized start angle $= 0.26 \pm 0.03$ relative to U) and laterally at the end of this phase (normalized end angle $= 0.55 \pm 0.06$). In contrast, downward swimmers initiated their power stroke medially (normalized start angle $= 0.52 \pm 0.05$) and terminated it posteriorly (normalized end angle $= 0.75 \pm 0.04$) (Table 1; Fig. 2). Other swimming parameters remained unaffected; upward and downward swimmers had comparable leg beat frequencies f, with the former averaging $f = 58.3 \pm 0.6$ s^{-1} and the latter $f = 59.5 \pm 1.8$ s^{-1}.

The orientation-based kinematics discussed above caused two distinct near-field flow structures (Figs. 1 and 2). Slow, upward-swimming copepods acted as *pullers*, entraining the water toward them, as seen with the flow converging anteriorly (Figs. 2c and d and 3). The pulling action of the cephalic appendages caused a local sharp drop in pressure anteriorly (Fig. 2g). In contrast, downward-swimming animals behaved as *pushers*, as evidenced by anterior fluid flow displacement in the swimming direction and the subsequent lateral deflection of the water (Figs. 2d and f and 3). This resulted in a local increase in pressure in front of the copepods (Fig. 2h). The shape and distribution of the induced vortices around the body also differed substantially. Upward swimmers produced vortex pairs on each side of the body; one large vortex lateral to the prosome (body) and another laterally compressed vortex extending posteriorly along the urosome (tail) (see Fig. 3). Fast, downward-cruising specimens also produced two vortices: one small vortex surrounding all the cephalic appendages and a much larger counter-rotating vortex located posteriorly and extending far behind the urosome (Fig. 2d and f). Note that the larger vortex forming in the upward and downward swimming cases have opposite signs.

In the case of upward swimming copepods, the anterior pressure fluctuations coincided with notable oscillations in the net thrust. Downward swimmers, however, generated nearly constant net thrust (Fig. 4). In general, the net thrust oscillated around zero over a complete beat cycle. This is expected because, by definition, during steady swimming, the thrust and drag forces – and the gravitational force in upward swimmers – are balanced, resulting in no net time-average acceleration. Upward swimmers generated positive net thrust throughout the entirety of the power stroke and the initial phase of the recovery stroke. Net drag was produced during the remainder of the leg recovery phase (Fig. 4e). Overall, the balance of forces (i.e., thrust and drag) was comparable between the two swimming cases during the power stroke. Dominant push forces were relatively constant during the first half of the power stroke and gradually dropped before initiating the recovery stroke (Fig. 4e and f). However, upward swimmers also produced positive net thrust at the beginning of the recovery stroke due to strong

pull forces at the front of the body (Fig. 4a). Net thrust was produced during 27.2 and 31.2% of the duration of the recovery stroke of copepods 8 and 5, respectively. This is consistent with the pulling behavior and anterior local pressure drop described above (Figs. 2 and 4c). Drag eventually dominated later in the recovery stroke due to the vortex developing along the prosome that entrained water posteriorly to the body, thus increasing pull drag. These effects were not present in the fast cruisers, as shown by the overall balance between these forces during the recovery stroke. In this case, at the beginning of the recovery stroke, the anterior flow was mostly dominated by positive pressure gradients, which generated drag (Figs. 2f and 4b and d). Note that the upward-swimming copepods have greater force coefficients than the downward swimmers. This is because the raw force magnitudes of both cases are equivalent, but upward copepods are slower. Thus, the latter would produce proportionally more force and potentially more power to achieve the same swimming speed as downward cruisers.

Discussion

Copepods and many other mesozooplankton species actively swim from the ocean surface down to several hundred meters deep and back up to avoid predation and feed (Marshall and Orr 1972; Roe 1972). In doing so, these organisms are subjected to external mechanical forces resisting swimming, such as drag and weight due to gravity. Gravity was identified by Clarke (Clarke 1934) as a critical factor in negatively buoyant plankters like *Temora longicornis*, which tend to sink continuously. Recent CFD-based empirical models show that the drag coefficient of a negatively buoyant, self-propelled copepod depends on the excess weight due to its overall contribution to the total swimming speed (Jiang 2023). This forces upward swimmers to induce a stronger velocity gradient than downward-swimming copepods to counteract these two retarding forces (Strickler 1982; Emlet and Strathman 1985). We found that this also contributes to stronger pressure gradients anteriorly. The literature reports how copepods often generate a funnel-shaped anterior flow prone to producing sub-ambient pressures (Tiselius and Jonsson 1990; Malkiel et al. 2003). This phenomenon is often tied to feeding and hovering, whereby copepods generate a stronger anterior current, facilitating prey capture and manipulation (Gerritsen and Strickler 1977; Jiang 2023). However, the link between pulling and pushing the water anteriorly and the swimming orientation has not been established in detail.

We found that the water just anterior to *T. longicornis* will either be pushed forward or pulled backward during cruising depending on their orientation with respect to the gravitational acceleration (see Figs. 2 and 3). Upward swimmers utilize a *pull-based* mechanism, whereas downwards swimmers use a *push-based* mechanism. The pulling mechanism plays an important role during feeding (i.e., increasing prey encounter rate and capture) and sensing (Kiørboe and Jiang 2013; Yen 2013; Kiørboe et al. 2014), but its role in locomotion, particularly during vertical relocation, remains to be explored. We present evidence that the onset of a strong pulling current works to drop the pressure directly in front of the copepods to enhance thrust when swimming upward (Fig. 4). Specifically, the reciprocal action of this sub-ambient pressure gradient anterior to the body does work on the body in the swimming direction (thus opposite to both drag and gravity), contributing to net thrust during about 30% of the leg recovery stroke, a phase normally dominated by drag. The inertia carried by the persisting induced flow can be harnessed at no additional cost and potentially offers negatively buoyant copepods an effective solution to overcome the combined effects of induced drag and excess weight. Here, we emphasize the role of inertial effects in thrust and drag production. Shear effects are also important, as seen with high vorticity along the prosome and urosome (Fig. 2). Theoretical models accounting for body drag and excess weight indicate that upward swimming is comparatively not as efficient as hovering and downward swimming because it requires more power (Jiang 2023). While cruising upward might be less energy efficient than downward swimming, copepods have evolved to take advantage of the inertial effects of the persistent, induced anterior flow. Despite slower swimming speeds, this strategy may help lower the COT compared with an upward pusher through the generation of additional thrust. On the other hand, acceleration reaction forces would contribute directly to drag, adding to the retarding moments of the excess weight and body drag. This highlights an important mechanism by which copepods may conserve energy during long vertical migrations, which can potentially have an important impact on the ecology and locomotion of other plankton species.

What causes the contrasting near-field flow structure of pullers and pushers? Following, we discuss how a subtle, yet necessary shift of the leg movements modulates the structure of the near-field flow and consequently affects the propulsive forces of pullers and pushers in the context of vertical cruising. The observed copepods consistently displayed a particular set of leg kinematics for a specific swimming direction, whereby the initial position of the swimming legs during a beat effectively modulates the flow direction. Pullers performed *breaststroke* kinematics consisting of the cephalic appendages extending anteriorly and creating a vacuum when displaced laterally during the power stroke (Fig. 2). In contrast, pushers produce much weaker pressure

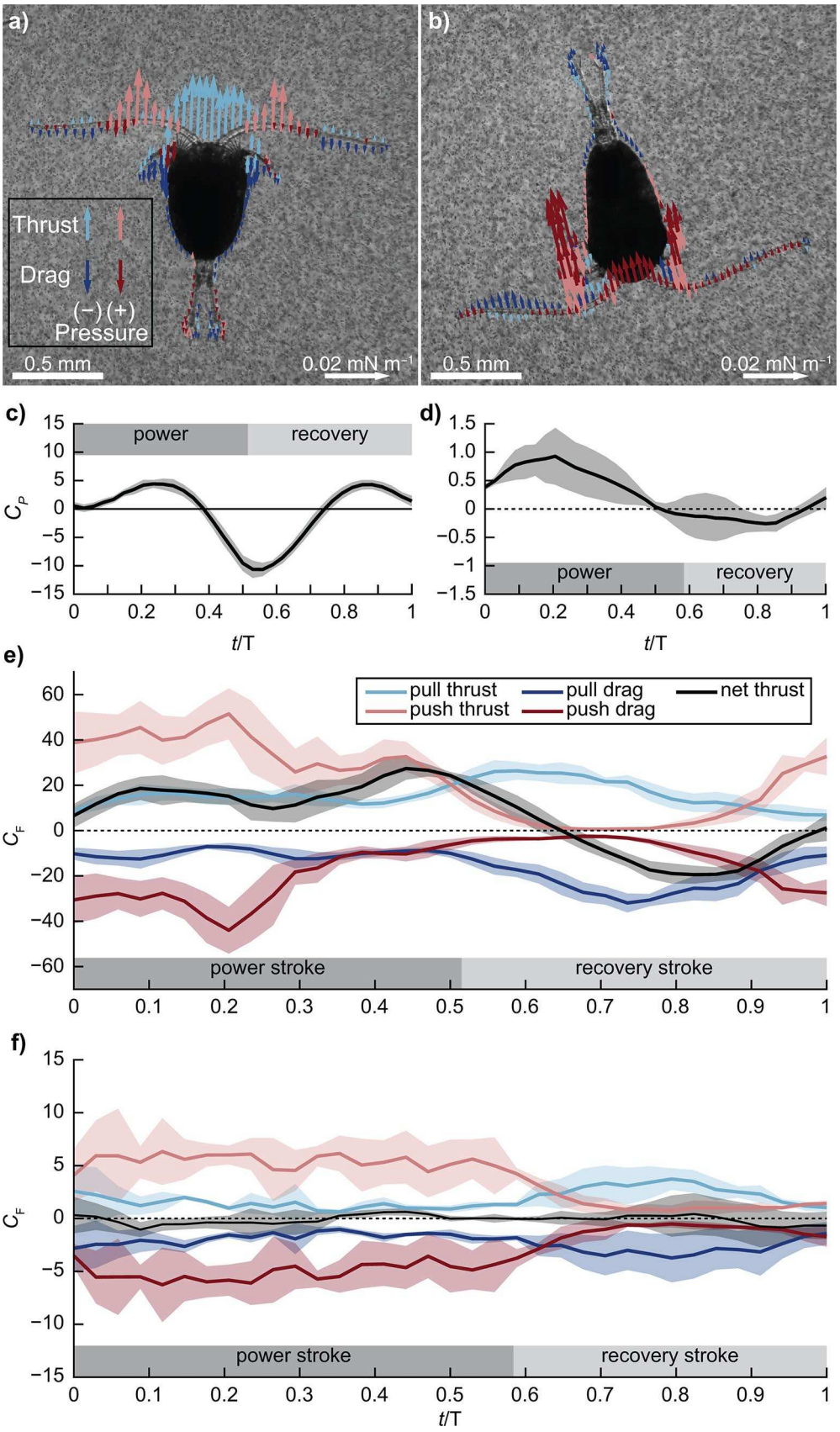
a)
b)
Thrust
Drag
(−) (+)
Pressure
0.5 mm
0.02 mN m⁻¹
0.5 mm
0.02 mN m⁻¹
c)
power
recovery
C_P
t/T
d)
power
recovery
t/T
e)
pull thrust
push thrust
pull drag
push drag
net thrust
C_F
power stroke
recovery stroke
f)
C_F
power stroke
recovery stroke
t/T

Fig. 4 Instantaneous forces produced during swimming for representative upward and downward swimmers. Instantaneous force vectors at the end of the power stroke for a representative slow, upward swimming (**a**) and a fast, downward swimming copepod (**b**). Only the axial component is plotted to show the net contribution to thrust and drag acting in the swimming direction. Every two vectors are plotted for clarity. The sign of the pressure coefficient (C_P) in front of upward swimmers (**c**) fluctuates twice during a beat cycle, while it changes only once in downward cruisers (**d**). Downward swimmers generate strong sub-ambient pressures at the beginning of the recovery stroke. (**e**) Mean instantaneous force coefficients (C_F) for the upward-swimming copepod depicted in (**a**) and (**c**). (**f**) Mean instantaneous C_F for the downward-swimming copepod depicted in (**b**) and (**d**). Solid lines in (**c–f**) indicate the mean for 10 and 3 leg beat cycles for each representative upward and downward swimmer, respectively, and shading shows the standard deviation. The time t during a stroke is normalized to the beat period T

gradients — with dominating positive pressures — because the initial lateral orientation of their swimming legs cannot induce a proper vacuum. An upside to this is that the pushers are less likely to waste energy laterally since the normal component of the force produced by the legs is oriented more axially compared with pullers. This simple change in the leg kinematics is sufficient to modulate the near-field flow and promote conditions favorable to harnessing suction forces to generate more thrust.

Given the significant benefits of pulling, why do downward-swimming copepods not adopt it? They no longer need to generate additional forces to overcome gravity, and only body drag opposes motion. In fact, the added effects of the excess weight contribute directly to increasing the overall swimming speed due to the terminal velocity (see Table 1)(Clarke 1934) and, at least partially, counter drag to produce thrust far more uniformly (Fig. 4). Compared with upward copepods needing to overcome the effects of their weight, this undoubtedly requires less power (Jiang 2023) and thus potentially lowers the COT, thereby promoting efficient, fast cruising. This is central to their natural DVM behavior, for which they swim to greater depths. Note that gravity does not oppose motion during horizontal swimming, thus still leaving drag as the only retarding force. As such, copepods are more likely to display the pushing behavior to swim faster. Our results indicate that even when a pronounced horizontal component exists, the swimming kinematics, induced flow, and forces are consistent with fast, downward pushers.

Copepods can still achieve fast swimming when not entirely assisted by gravity. However, whether behaving as pullers would be more advantageous in this context is unclear. Suction-based thrust might still be less efficient than cruising as a pusher with (or even without) the help of gravity. For this reason, pulling may be undesirable. Nonetheless, the pulling behavior demonstrates important benefits of enhancing thrust when needing to overcome negative buoyancy. One question remains unanswered, however: is an upward-swimming, pulling copepod more efficient than the same but otherwise pushing copepod? This may not be easily addressed experimentally, but computational fluid dynamics models can compare the energetics of upward- and downward-cruising pullers and pushers and quantify the impact of this suction-based pulling behavior on DVM.

Future research using a more diverse range of copepod species would provide valuable additional insights and potentially extend the patterns observed in this study. Still, our results provide new insights into important hydrodynamic mechanisms at the organismal level, whose cumulative effects in large aggregations during DVMs can potentially impact the vertical distribution of marine biogeochemical properties by enabling a large biomass to migrate through the water column and potentially induce large-scale bio-induced flows. We anticipate integrating these findings into global circulation models with realistic ocean biogeochemistry, including the hydrodynamic effects of swimming aggregations, will shed light on the role of biogenic hydrodynamic transport in redistributing nutrients, oxygen, and carbon in the upper ocean. Our work shows that copepods modulate the near-body flow in response to their orientation in the water column, which has important repercussions in the context of transport and mixing as numerical simulations often discretize fluid-structure interactions based on a single swimmer type (pusher or puller) and do not account for changes based on orientation.

Acknowledgements We are grateful to Yunxing Su for his insightful input during the conceptualization of this research and his comments on the initial draft. We also thank the anonymous reviewers of our manuscript for their valuable feedback. We gratefully acknowledge the contribution of Rose Weinbaum in the creation of manual copepod masks.

Author contributions Conceptualization: S.O.S, M.M.W, B.J.G.; Methodology: N.B.T, S.O.S., M.M.W., B.J.G.; Software: N.B.T, S.O.S; Validation: N.B.T.; Formal analysis: N.B.T.; Investigation: N.B.T., S.O.S, B.J.G., M.M.W.; Resources: M.M.W., B.J.G.; Writing - original draft: N.B.T.; Writing - review and editing: N.B.T, S.O.S, M.M.W, B.J.G.; Visualization: N.B.T; Funding acquisition: M.M.W., B .J.G.

Funding This work was partially supported by the National Aeronautics and Space Administration Ocean Biology and Biogeochemistry Program (MMW, grant number 80NSSC22K0284). Funding for this project was provided by the National Science Foundation OCE-1829945 and CBET- 2100703 to BJG.

Data availability The copepod data and metadata reported in this investigation have been deposited in the Brown University Digital Repository: https://doi.org/10.26300/mfeq-2w97. Custom Matlab scripts developed to compute and analyze forces from experimentally derived pressure fields were also deposited in this repository.

Declarations

Ethical approval All copepod sampling and experiments were conducted in accordance with the laws of the State of Rhode Island and research ethics and integrity policies of Brown University and the University of South Florida.

Conflict of interest The authors declare no competing interests.

References

Apstein C (1910) Hat ein Organismus in Der Tiefe Gelebt, in Der Er gefischt ist. Int Revue Der Gesamten Hydrobiol Und Hydrographie 3:17–33. https://doi.org/10.1002/iroh.19100030109

Archibald KM, Siegel DA, Doney SC (2019) Modeling the impact of zooplankton diel vertical migration on the carbon export flux of the biological pump. Global Biogeochem Cy 33:181–199. https://doi.org/10.1029/2018GB005983

Aumont O, Maury O, Lefort S, Bopp L (2018) Evaluating the potential impacts of the diurnal vertical migration by marine organisms on marine biogeochemistry. Global Biogeochem Cy 32:1622–1643. https://doi.org/10.1029/2018GB005886

Bianchi D, Stock C, Galbraith ED, Sarmiento JL (2013) Diel vertical migration: ecological controls and impacts on the biological pump in a one-dimensional ocean model. Global Biochem Cy 27:478–491. https://doi.org/10.1002/gbc.20031

Bianchi D, Mislan K, a. S (2016) Global patterns of diel vertical migration times and velocities from acoustic data. Limnol Oceanogr 61:353–364. https://doi.org/10.1002/lno.10219

Bundy MH, Paffenhöfer GA (1996) Analysis of flow fields associated with freely swimming calanoid copepods. Mar Ecol Prog Ser 133:99–113. https://doi.org/10.3354/meps133099

Cannon HG (1928) On the feeding mechanism of the copepods, *Calanus finmarchicus* and *Diaptomus Gracilis*. J Exp Biol 6:131–144. https://doi.org/10.1242/jeb.6.2.131

Cavan EL, Laurenceau-Cornec EC, Bressac M, Boyd PW (2019) Exploring the ecology of the mesopelagic biological pump. Prog Oceanogr 176:102125. https://doi.org/10.1016/j.pocean.2019.102125

Clarke GL (1934) Factors affecting the vertical distribution of copepods. Ecol Monogr 4:530–540. https://doi.org/10.2307/1961656

Colin SP, Costello JH, Dabiri JO, Villanueva A, Blottman JB, Gemmell BJ, Priya S (2012) Biomimetic and live medusae reveal the mechanistic advantages of a flexible bell margin. PLoS ONE 7:e48909. https://doi.org/10.1371/journal.pone.0048909

Colin SP, Costello JH, Sutherland KR, Gemmell BJ, Dabiri JO, Du Clos KT (2020) The role of suction thrust in the metachronal paddles of swimming invertebrates. Sci Rep 10:17790. https://doi.org/10.1038/s41598-020-74745-y

Conroy JA, Steinberg DK, Thibodeau PS, Schofield O (2020) Zooplankton diel vertical migration during Antarctic summer. Deep Sea Res Pt I 162:103324. https://doi.org/10.1016/j.dsr.2020.103324

Dabiri JO, Bose S, Gemmell BJ, Colin SP, Costello JH (2014) An algorithm to estimate unsteady and quasi-steady pressure fields from velocity field measurements. J Exp Biol 217:331–336. https://doi.org/10.1242/jeb.092767

Dabiri JO, Colin SP, Gemmell BJ, Lucas KN, Leftwich MC, Costello JH (2020) Jellyfish and fish solve the challenges of turning dynamics similarly to achieve high maneuverability. Fluids 5:106. https://doi.org/10.3390/fluids5030106

Emlet RB, Strathman RR (1985) Gravity, drag, and feeding currents of small zooplankton. Science 228:1016–1017. https://doi.org/10.1126/science.228.4702.1016

Gauld DT (1953) Diurnal variations in the grazing of planktonic copepods. J Mar Biol Assoc UK 31:461–474. https://doi.org/10.1017/S0025315400011619

Gemmell BJ, Adhikari D, Longmire EK (2014) Volumetric quantification of fluid flow reveals fish's use of hydrodynamic stealth to capture evasive prey. J R Soc Interface 11:20130880. https://doi.org/10.1098/rsif.2013.0880

Gemmell BJ, Colin SP, Costello JH, Dabiri JO (2015) Suction-based propulsion as a basis for efficient animal swimming. Nat Commun 6:1–8. https://doi.org/10.1038/ncomms9790

Gemmell BJ, Fogerson SM, Costello JH, Morgan JR, Dabiri JO, Colin SP (2016) How the bending kinematics of swimming lampreys build negative pressure fields for suction thrust. J Exp Biol 219:3884–3895. https://doi.org/10.1242/jeb.144642

Gerritsen J, Strickler JR (1977) Encounter probabilities and community structure in zooplankton: a mathematical model. J Fish Res Board Can 34:73–82. https://doi.org/10.1139/f77-008

Giuffre C, Hinow P, Jiang H, Strickler JR (2019) Oscillations in the near-field feeding current of a calanoid copepod are useful for particle sensing. Sci Rep 9:17742. https://doi.org/10.1038/s41598-019-54264-1

Haury L, Weihs D (1976) Energetically efficient swimming behavior of negatively buoyant zooplankton. Limnol Oceanogr 21:797–803. https://doi.org/10.4319/lo.1976.21.6.0797

Houghton IA, Dabiri JO (2019) Alleviation of hypoxia by biologically generated mixing in a stratified water column. Limnol Oceanogr 64:2161–2171. https://doi.org/10.1002/lno.11176

Houghton IA, Koseff JR, Monismith SG, Dabiri JO (2018) Vertically migrating swimmers generate aggregation-scale eddies in a stratified column. Nature 556:7702: 497–500. https://doi.org/10.1038/s41586-018-0044-z

Humes AG (1994) How many copepods? Hydrobiologia 292/. 293:1–7. https://doi.org/10.1007/BF00229916

Jiang H (2002) The flow field around a freely swimming copepod in steady motion. Part I: theoretical analysis. J Plankton Res 24:167–189. https://doi.org/10.1093/plankt/24.3.167

Jiang H (2023) The swim-and-sink behaviour of copepods: a revisit to mechanical power requirement and a new hypothesis on function. R Soc Open Sci 10:230347. https://doi.org/10.1098/rsos.230347

Jiang H, Osborn TR (2004) Hydrodynamics of copepods: a review. Surv Geophys 25:339–370. https://doi.org/10.1007/s10712-003-1282-6

Kiørboe T, Jiang H (2013) To eat and not be eaten: optimal foraging behaviour in suspension feeding copepods. J R Soc Interface 10:20120693. https://doi.org/10.1098/rsif.2012.0693

Kiørboe T, Jiang H, Gonçalves RJ, Nielsen LT, Wadhwa N (2014) Flow disturbances generated by feeding and swimming zooplankton. P Natl Acad Sci 111:11738–11743. https://doi.org/10.1073/pnas.1405260111

Lucas KN, Dabiri JO, Lauder GV (2017) A pressure-based force and torque prediction technique for the study of fish-like swimming. PLoS ONE 12:e0189225. https://doi.org/10.1371/journal.pone.0189225

Malkiel E, Sheng J, Katz J, Strickler JR (2003) The three-dimensional flow field generated by a feeding calanoid copepod measured using digital holography. J Exp Biol 206:3657–3666. https://doi.org/10.1242/jeb.00586

Marshall SM, Orr AP (1972) Vertical migration. In: Marshall SM (ed) The Biology of a Marine Copepod *Calanus finmarchicus* (Gunnerus). Springer, Berlin, Heidelberg, pp 123–141

Mauchline J (1998) Behaviour. In: Blaxter J (ed) The biology of calanoid copepods. Academic, London, London, UK, pp 400–455

Roe HSJ (1972) The vertical distributions and diurnal migrations of calanoid copepods collected on the SOND Cruise, 1965 I. The total population and general discussion. J Mar Biol Assoc UK 52:277–314. https://doi.org/10.1017/S0025315400018713

Schneider C, Rasband W, Eliceiri K (2012) NIH Image to ImageJ: 25 years of image analysis. Nat Methods 671–675. https://doi.org/10.1038/nmeth.2089

Siegel DA, DeVries T, Cetinić I, Bisson KM (2023) Quantifying the ocean's biological pump and its carbon cycle impacts on global scales. Annu Rev Mar Sci 15:329–356. https://doi.org/10.1146/annurev-marine-040722-115226

Steinberg DK, Landry MR (2017) Zooplankton and the ocean carbon cycle. Annu Rev Mar Sci 9:413–444. https://doi.org/10.1146/annurev-marine-010814-015924

Strickler JR (1982) Calanoid copepods, feeding currents, and the role of gravity. Science 218:158–160. https://doi.org/10.1126/science.218.4568.158

Strickler JR (1984) Sticky water: a selective force in copepod evolution. In: Meyer D, Strickler J (eds) Trophic interactions within aquatic ecosystems. Routledge, pp 187–239

Svetlichny L, Larsen P, Kiørboe T (2020) Kinematic and dynamic scaling of copepod swimming. Fluids 5:68. https://doi.org/10.3390/fluids5020068

Tack NB, Du Clos KT, Gemmell BJ (2021) Anguilliform locomotion across a natural range of swimming speeds. Fluids 6:127. https://doi.org/10.3390/fluids6030127

Tiselius P, Jonsson PR (1990) Foraging behaviour of six calanoid copepods: observations and hydrodynamic analysis. Mar Ecol Prog Ser 66:23–33

Wilhelmus MM, Dabiri JO (2014) Observations of large-scale fluid transport by laser-guided plankton aggregations. Phys Fluids 26:101302. https://doi.org/10.1063/1.4895655

Wilhelmus MM, Nawroth J, Rallabandi B, Dabiri JO (2019) Effect of swarm configuration on fluid transport during vertical collective motion. Bioinspir Biomim 15:015002. https://doi.org/10.1088/1748-3190/ab435b

Yen J (2013) Appendage diversity and modes of locomotion: swimming at intermediate Reynolds numbers. In: Watling L, Thiel M (eds) Functional morphology and diversity. Oxford University Press, pp 297–318

Yen J, Strickler JR (1996) Advertisement and concealment in the plankton: what makes a copepod hydrodynamically conspicuous? Invertebr Biol 15:191–205. https://doi.org/10.2307/3226930